HHS Public Access

Author manuscript

Neuroimage. Author manuscript; available in PMC 2022 April 15.

Published in final edited form as:

Neuroimage. 2022 April 15; 250: 118939. doi:10.1016/j.neuroimage.2022.118939.

Individual predictors and electrophysiological signatures of working memory enhancement in aging

Elizabeth L. Johnson[a,1,*], **Hector Arciniega**[b,1], **Kevin T. Jones**[c], **Alexandrea Kilgore-Gomez**[d], **Marian E. Berryhill**[d,*]

[a]Departments of Medical Social Sciences and Pediatrics, Northwestern University, Chicago, IL, 60611, United States

[b]Psychiatry Neuroimaging Laboratory, Brigham and Women's Hospital, Harvard Medical School, Boston, MA, 02215, United States

[c]Department of Neurology, Neuroscape, University of California-San Francisco, San Francisco, CA, 94158, United States

[d]Department of Psychology, Program in Cognitive and Brain Sciences, Program in Integrative Neuroscience, University of Nevada, Reno, 89557, United States

Abstract

A primary goal of translational neuroscience is to identify the neural mechanisms of age-related cognitive decline and develop protocols to maximally improve cognition. Here, we demonstrate *how* interventions that apply noninvasive neurostimulation to older adults improve working memory (WM). We found that one session of sham-controlled transcranial direct current stimulation (tDCS) selectively improved WM in older adults with more education, extending earlier work and underscoring the importance of identifying individual predictors of tDCS responsivity. Improvements in WM were associated with two distinct electrophysiological signatures. First, a broad enhancement of theta network synchrony tracked improvements in behavioral accuracy, with tDCS effects moderated by education level. Further analysis revealed that accuracy dynamics reflected an anterior-posterior network distribution regardless of cathode placement. Second, specific enhancements of theta-gamma phase-amplitude coupling (PAC) reflecting tDCS current flow tracked improvements in reaction time (RT). RT dynamics further explained inter-individual variability in WM improvement independent of education. These findings illuminate theta network synchrony and theta-gamma PAC as distinct but complementary mechanisms supporting WM in aging. Both mechanisms are amenable to intervention, the effectiveness of which can be predicted by individual demographic factors.

*Corresponding authors. eljohnson@northwestern.edu (E.L. Johnson), mberryhill@unr.edu (M.E. Berryhill).
[1]Denotes equal contribution as co-first authors.

Declaration of Competing Interest

The authors declare no competing financial interests.

Supplementary materials

Supplementary material associated with this article can be found, in the online version, at doi:10.1016/j.neuroimage.2022.118939.

Keywords

Aging; EEG; Individual differences; tDCS; Theta; Working memory

1. Introduction

Older adults (OA) with preserved working memory (WM) maintain independence in their daily lives, such as remembering to turn off the oven after use, take medications, and balance their checkbooks (Buckner, 2004). Unfortunately, WM declines as we age, with cognitive performance peaking in our 20 s (Park et al., 2002; Reuter-Lorenz and Sylvester, 2005). This age-related WM decline arises from age-related reductions in the brain's cortical thickness (Salat et al., 2004), structural connectivity (Cabeza, 2001), and functional connectivity (Courtney and Hinault, 2021). Recent efforts augmenting cognitive training with non-invasive neuromodulatory approaches, such as transcranial direct current stimulation (tDCS), have demonstrated that multi-session tDCS can improve WM with low risk and cost (Berryhill, 2017; Berryhill and Martin, 2018). Indeed, we demonstrated that multi-session tDCS improved WM in OA, with benefits persisting one month after the last stimulation session (Jones et al., 2015b). Such successes hold promise for clinical and commercial endeavors aiming to halt age-related cognitive decline without pharmacological intervention (Polanía et al., 2018). However, single-session tDCS studies are rife with inter-individual variability in cognitive performance outcomes (Berryhill and Martin, 2018), impeding widespread implementation. We address this discrepancy and provide a mechanistic account of how, and in whom, one session of tDCS improves WM in healthy OA at risk of cognitive decline.

TDCS affects the brain in a variety of ways, including measurable effects on resting neuronal potentials (Nitsche and Paulus, 2001) and neuroplasticity (Filmer et al., 2014), resting-state functional connectivity (Kim et al., 2021; Nissim et al., 2020, 2019), glutamate levels (Mezger et al., 2019), and neural oscillations (Jones et al., 2020a,b, 2017; Luft et al., 2018; Reinhart et al., 2015). The acute effects of tDCS on resting neuronal potentials persist for ~60 min (Nitsche and Paulus, 2001), and multi-session tDCS effects in the electroencephalogram (EEG) persist for at least 24 h concurrent with WM enhancement (Jones et al., 2020a, 2017). Such proof-of-concept work in healthy young adults has associated tDCS-linked WM gains with enhancements of anterior-posterior functional connectivity, particularly in the theta band (Gan et al., 2019; Jones et al., 2017; Zaehle et al., 2011), and theta-gamma phase amplitude coupling (PAC) (Jones et al., 2020a). It is therefore reasonable to hypothesize that tDCS-linked WM gains in OA would likewise be associated with anterior-posterior theta connectivity and theta-gamma PAC. This proposal is supported by recent research directly manipulating theta oscillations in OA (Reinhart and Nguyen, 2019), suggesting a causal brain-behavior link.

To test this hypothesis, we conducted a systematic investigation of individual predictors and electrophysiological mechanisms of WM enhancement in healthy OA after one session of sham-controlled tDCS. The design was based in part on an earlier influential study where we observed that OA with more education selectively improved after one dose of anodal

tDCS targeting left or right prefrontal cortex (PFC) (Berryhill and Jones, 2012). More recent work showed that changing the montage to target right PFC and posterior parietal cortex (PPC) may be more effective in OA with lower scores on standardized measures of WM span (Arciniega et al., 2018). These selective benefits confirm that null findings derived from the whole sample (e.g., Nilsson et al., 2015) obscure pertinent individual differences (Medina and Cason, 2017; Polanía et al., 2018). Thus, the present study investigated several individual differences factors, including education level and standardized WM span, and two tDCS montages: anode right PFC-cathode right PPC (Arciniega et al., 2018) and anode right PFC-cathode contralateral cheek (CC) (Berryhill and Jones, 2012). In addition, our WM task's high trial count (n = 576) permitted analysis of tDCS effects across the ~60-min post-stimulation session and ensured stable EEG data at the individual level. Preempting the results, analyses of behavioral accuracy and reaction time (RT) (Brooks et al., 2020; Cerreta et al., 2020; Jones et al., 2020a, 2017; Martin et al., 2017; Reinhart et al., 2017b) identified an individual's education level as the most robust predictor of tDCS efficacy across montages. Subsequent EEG analyses determined the mechanisms underlying individual behavioral improvements (Finn and Rosenberg, 2021; Krakauer et al., 2017). Results converged to reveal high inter-individual variability underpinned by nuanced mechanisms, explaining how tDCS improved WM in OA with more education *and* suggesting an alternate route by which OA with less education could still benefit.

2. Materials and methods

2.1. Participants

Thirty right-handed OA participated (17 females and 13 males; mean ± SD, age: 67.33 ± 3.57 years; education: 16.37 ± 2.04 years, range 12–20 years). Screening excluded those with neurological or psychiatric disorders, head injuries, prescriptions for neuroleptic, hypnotic, or anti-seizure medications, or a score of < 26 on the Montreal Cognitive Assessment (MOCA; version 7.1). Procedures were approved by the University of Nevada Institutional Review Board in accordance with the Declaration of Helsinki. Participants signed consent documents and received $15/hour.

2.2. Experimental design

2.2.1. Baseline measures—During baseline testing, participants completed the Corsi Blocks Spatial Span (CORSI; MATRICS Consensus Cognitive Battery; Nuechterlein et al., 2008), Digit Span (Wechsler, 2009), and automated Operation Span (OSpan; Unsworth et al., 2005) assessments of WM capacity. Correlations between demographic and baseline measures indicated a significant inverse correlation between age and OSpan (Table S1), without other significant effects. In this sample, education was independent of WM ability (Berryhill and Jones, 2012).

2.2.2. Visual change detection WM task—During three tDCS sessions, participants completed a visual change detection WM task (Arciniega et al., 2019, 2020, 2021; Vogel and Machlzawa, 2004); Fig. 1A, B). Participants sat 57 cm from the monitor and were instructed to maintain fixation and avoid eye movements. Color patch stimuli (0.7° × 0.7°; cyan, white, red, blue, yellow, green, magenta) were presented at three possible locations

4.6° to either side of fixation (0.4° × 0.4°) against a uniform gray background. Trials began with fixation (0.4° × 0.4°; 0.3 s), followed by an attentional cue (arrow-head: 2.1° × 0.4°; 0.2 s) indicating which hemifield to covertly attend. After a stimulus onset asynchrony delay (SOA; 0.3–0.4 s), one or three stimuli flashed per hemifield (0.1 s), followed by a delay (0.9 s) and the probe stimulus (3 s). Participants indicated via keypress whether the color of the encoded and probe stimuli within the cued hemifield matched (50% match). No feedback was provided. During stimulation, participants completed 72 practice trials. During EEG, participants completed 576 trials with self-paced breaks between quartiles (144 trials). The task was counterbalanced across sessions, set sizes, and attended hemifields. The task was programmed using PsychToolbox (Brainard, 1997) for MATLAB (MathWorks, Inc., Natick, MA).

2.2.3. TDCS protocol—TDCS was applied using two montages in a fully within-subjects, sham-controlled design (Fig. 1C, D). TDCS (two 5 × 7 cm^2 electrodes in saline-dampened sponges) was applied using a constant current stimulator (Eldith Magstim, GmbH, Ilmenau, Germany). There were two electrode montages: PFC-PPC (anode F6, cathode P6) and PFC-CC (anode F6, cathode CC). Current modeling was conducted using the Realistic volumetric Approach to Simulate Transcranial Electric Stimulation (ROAST) toolbox for the anode location (F6) and both cathode locations (P6, CC) on the MNI-152 standard head (Huang et al., 2018). Cathode placement was counterbalanced for sham testing (Gandiga et al., 2006). All tDCS montages were evenly counterbalanced to ensure proper distributions, with a third of participants assigned to sham, PFC-PPC tDCS, and PFC-CC tDCS on each day of the three-day experiment (Arciniega et al., 2018; Berryhill et al., 2010; Jones and Berryhill, 2012; Jones et al., 2015a; Tseng et al., 2012). Sessions were separated by a 24-h washout. Participants were blinded to the session condition.

2.2.4. EEG data acquisition and preprocessing—High-density EEG was recorded at a sampling rate of 1 kHz with a vertex (Cz) reference from 256 high-impedance electrodes mounted in a HydroCel Geodesic Sensor Net amplified by a Net Amps 300 amplifier. Data were acquired using Net Station 5.2 software (Electrical Geodesics Inc., Eugene, OR) running on a 2.7 GHz dual-core Apple Power Mac G5. Electrode impedances were kept below 50 K Ω. Raw EEG data were bandpass filtered (0.5–100 Hz Butterworth infinite impulse response filter) and 60-Hz line noise was removed using discrete Fourier transform. Data were inspected to reject artifactual channels (e.g., from signal dropout), down-sampled to 250 Hz, and segmented into 3-s trials (−1 to + 2 s from stimulus onset). Independent components analysis removed artifacts (i.e., eye movements, auricular components, heartbeat, and cranial muscle activity; Hipp and Siegel, 2013). Channels on the face, ears, and neck were discarded and any rejected channels were replaced with interpolated mean values from neighboring channels (mean 7.4 channels). The remaining 194 channels were reinspected blind to task parameters to reject trials containing residual noise. The surface Laplacian spatial filter was applied to minimize volume conduction and enhance the high-density source signal (Cohen, 2015; He et al., 2018; Lai et al., 2018). Error trials were excluded (Jones et al., 2017), resulting in a mean of 443 (SD: 40) artifact-free, correct trials analyzed per session. EEG preprocessing and analysis routines utilized functions from the open-source FieldTrip toolbox for MATLAB (Oostenveld et al., 2011).

2.2.5. Spectral decomposition—Laplacian-transformed data segments were zero-padded to 10 s to minimize filtering-induced edge artifacts and bandpass filtered per channel at 20 logarithmically spaced, partially overlapping frequencies centered from 2 to 60 Hz (1/3 fractional bandwidth). The Hilbert transform was used to extract the analytic amplitude envelope from each filtered time series, which was squared to produce power. SOA (−0.3–0 s from stimulus onset) and delay power time series (0.1–1 s from stimulus onset) were then corrected on the pre-cue baseline (−0.8 to −0.6 s from stimulus onset) to derive event-related spectral perturbations (ERSPs): ERSPs = (SOA or delay − baseline mean)/baseline mean (Jones et al., 2017). Outputs were averaged over the SOA and delay epochs to derive mean ERSPs in single trials.

2.2.6. Network synchrony—Laplacian-transformed data segments were zero-padded to 10 s and bandpass filtered per channel at a subset of logarithmically spaced frequencies centered from 2 to 20 Hz following removal of the event-related potential (ERP; Jones et al., 2020b, 2017). The filtered data were epoched over the delay (0.1–1 s from stimulus onset) and the Hilbert transform was used to extract instantaneous phase values from each filtered time series. Phase synchrony was quantified in single trials as phase-locking values (PLV) independent of amplitude (Lachaux et al., 1999). This method calculates the consistency in channel-pair phase differences across a series of data points, here, time points in single trials.

We used graph theory to map the topographical distributions of PLV networks in single trials. According to graph theory, brain networks are collections of nodes (here, Laplacian-transformed channels) and internode edges (PLV), summarized as adjacency matrices (Sporns, 2018). To define PLV adjacency matrices, PLV outputs were assessed for network degrees (i.e., the weight of connections between each channel and all other channels) using a threshold of 0.65 relative to the maximum of 1 (Jones et al., 2020b). All analyses were performed on network synchrony data. We selected this approach based on our prior work showing that tDCS enhances task-relevant PLV networks in young adults (Jones et al., 2020b). Furthermore, treating functional connectivity data as graph theoretical networks permits analysis of groups of three or more units and better captures the real-world system of the brain than do binary interactions between channel pairs (Battiston et al., 2021).

2.2.7. Phase-amplitude coupling—Laplacian-transformed data segments were zero-padded to 10 s and bandpass filtered per channel at logarithmically spaced frequencies centered from 2 to 20 Hz and at the broadband gamma (30–70 Hz) range following removal of the ERP (Jones et al., 2020a,b). The filtered data were epoched over the delay (0.1–1 s from stimulus onset) and z-scored per trial in the time domain to control for differences in voltage between trials. The Hilbert transform was used to extract the amplitude envelope from the gamma time series and then the gamma data were bandpass filtered a second time at logarithmically spaced frequencies centered from 2 to 20 Hz. The Hilbert transform was used to extract instantaneous phase values from both the low frequency and low frequency-filtered gamma time series. PAC was calculated between low-frequency phase at the PFC anodal site (F6) and low frequency-filtered gamma at all channels as PLV independent of low-frequency amplitude (Penny et al., 2008). We selected this approach based on our

prior work showing that tDCS-linked WM enhancement is related to PAC with theta phase at the PFC anodal site in young adults (Jones et al., 2020a). By considering whole-brain gamma, this approach replicated our prior work and permitted analysis of groups of three or more units. As in network synchrony analysis (see Section 2.2.6), PLV calculations were performed across time points in single trials.

2.3. Statistical analyses

2.3.1. TDCS-linked change within subjects—To quantify within-subject change and minimize between-subject variability, we analyzed normalized difference indices for behavioral task performance (WM accuracy, RT) and EEG measures (ERSPs, network synchrony, PAC): Difference Index (DI) = (tDCS mean − sham mean)/(tDCS mean + sham mean). This normalization formula outputs the individual within-subject effect of each tDCS montage relative to sham stimulation (Arciniega et al., 2018; Jones et al., 2020b, 2015b).

2.3.2. Inter-individual differences in tDCS-linked change—Initial analyses of behavior (DI WM accuracy, DI RT) tested for main effects and interactions of tDCS across montages (PFC-PPC, PFC-CC), set sizes (1, 3), and quartiles (Q1–4) using repeated measures ANOVAs compared to zero. Violations of sphericity were Greenhouse-Geisser corrected. Subsequent ANCOVAs assessed main effects of individual difference factors (age, education, MOCA, Digit Span, OSpan, CORSI) and interactions with tDCS montage. Behavioral analyses were conducted using the open-source JASP software (JASP Team, 2020. JASP Version 0.14.1 [Computer software]).

Electrophysiological signatures of changes in behavior were identified per tDCS montage using Spearman's rank correlation, ρ_{XY}, with X set to the DI EEG measure and Y set to the DI behavioral measure, cluster-corrected for multiple comparisons (Maris and Oostenveld, 2007). Clusters were formed in space and frequency by thresholding correlations at $p < 0.05$ using the maximum size criterion. Permutation distributions were generated by randomly shuffling data labels (1,000 iterations) and corrected p-values were obtained by comparing the observed data to the random permutation distributions. This is an extremely powerful approach because it recreates any biases in the data with each randomization and tests for brain-behavior correlations without any assumptions about their spatial or spectral distribution. Cluster-based statistics were conducted using the FieldTrip toolbox for MATLAB (Oostenveld et al., 2011).

Post hoc multiple regression analyses synthesized the observed individual predictors and electrophysiological signatures of WM and RT improvements. These analyses tested whether changes in EEG measures, averaged across cluster-corrected data points, and changes in behavior were moderated by education level, controlling for other individual differences factors (age, MOCA, Digit Span, OSpan, CORSI). Bootstrapping determined unstandardized regression coefficients (b) and 95% CI (1,000 iterations), as implemented in JASP.

2.3.3. Data-driven analysis of tDCS-linked change over time—A data-driven analysis of tDCS effects over time investigated the topographical distribution of theta network synchrony as a mechanism of WM improvement in aging. Trial-by-trial changes

in WM performance relative to sham (DI WM accuracy) were computed by calculating the proportion of correct trials in sliding trial windows of 100 trials shifted in steps of one trial (Tort et al., 2009). Trial-by-trial changes in theta network synchrony relative to sham (DI theta network synchrony) were obtained by calculating theta network synchrony across correct trials in the same 100-trial window. Note that DI scores were computed per 100-trial window by normalizing the tDCS mean on the sham mean (see Section 2.3.1). DI data were averaged across participants and the relationship between DI WM accuracy and DI theta network synchrony was analyzed over time using Spearman's rank correlation with cluster-based correction for multiple comparisons (see Section 2.3.2).

3. Results

3.1. Behavioral accuracy

3.1.1. Education level predicts WM improvement—To facilitate comparison with existing tDCS findings, we first evaluated changes in performance without considering individual differences. DI WM accuracy scores were subjected to a repeated measures ANOVA compared to zero including the within-subjects factors of montage (PFC-PPC, PFC-CC), set size (1, 3), and quartile (Q1–4). No main effects or interactions reached significance ($p > 0.13$; Fig. 2 A). Note that although there was no significant effect of set size on changes in WM, analysis of the raw data confirmed that the set size manipulation was effective across tDCS conditions, including sham (paired *t*-test $p < 0.001$; Fig. S1A).

To identify which individual differences factors would predict tDCS-linked WM improvement, we next incorporated individual differences to identify specific factors associated with tDCS efficacy. DI WM accuracy scores were subjected to an ANCOVA with the same within-subjects factors as the ANOVA (montage, set size, quartile) and six covariates: education, age, MOCA, Digit Span (Forward + Backward), OSpan, and CORSI (Forward + Backward). There was a significant contribution of education ($F_{1, 462} = 11.77$, $p < 0.001$, $\eta^2_p = 0.03$), such that *individuals with more education showed greater WM improvement* after tDCS (Fig. 2 B). In addition, there was a significant positive association with baseline WM ability as indexed by Digit Span ($F_{1, 462} = 8.70$, $p = 0.003$, $\eta^2_p = 0.02$) and a Digit Span × montage interaction ($F_{1, 462} = 4.92$, $p = 0.027$, $\eta^2_p = 0.01$). However, a significant interaction of OSpan × montage ($F_{1, 462} = 4.87$, $p = 0.028$, $\eta^2_p = 0.01$) revealed that baseline WM span measures predicted PFC-CC tDCS benefits in opposing directions, with Digit Span positively associated and OSpan negatively associated with WM improvement (Fig. 2C). In contrast, PFC-PPC tDCS was beneficial regardless of baseline WM abilities. No other effects reached significance ($p > 0.05$).

3.1.2. Theta network synchrony tracks WM improvement in OA with more education—Having demonstrated inter-individual differences in tDCS-linked WM improvement, we next sought underlying neural correlates. This analysis builds on our previous findings associating frontoparietal tDCS with enhanced theta synchrony and theta-gamma PAC in young adults (Jones et al., 2020a, 2017). Here, we tested whether these measures correlated with *individual* WM improvements. A significant cluster-corrected correlation between DI WM accuracy and DI network synchrony scores revealed network

enhancement in OA who benefitted from PFC-PPC tDCS (mean $\rho = 0.452$, $p = 0.031$; Fig. 3 A). The behavioral benefit was characterized by increased theta network synchrony (2–5.9 Hz) broadly distributed across the EEG topography, that is, more densely connected theta networks in OA who benefited more from PFC-PPC tDCS. The same analysis of changes associated with PFC-CC tDCS also returned a positive correlation, but it was weaker and failed cluster-based correction for multiple comparisons (mean $\rho = 0.411$, $p = 0.179$; Fig. 3 B). The correlations between DI WM accuracy and DI PAC scores (phase at the F6 anodal site and whole-brain gamma) were not significant for either montage ($p > 0.44$). For completeness, we also examined ERSPs and observed no significant correlations ($p > 0.21$).

Post hoc multiple regression analysis examined whether changes in theta network synchrony and WM accuracy after PFC-PPC tDCS were moderated by an individual's education level. A significant interaction between education and theta network synchrony revealed that individuals with more education improved more and showed greater enhancement of theta network synchrony ($t = 2.61$, $p = 0.016$, $b = 0.58$, 95% CI = [−0.34, 1.35]). Collectively, these results demonstrate that tDCS improved WM by enhancing theta networks, and the effect was robust with the PFC-PPC montage but not with the PFC-CC montage. Education moderated the relationship between changes in WM accuracy and theta network synchrony after PFC-PPC tDCS.

3.1.3. The theta network signature of WM improvement is distributed across anterior and posterior topographies—

The above results suggest that PFC-PPC tDCS more effectively targeted distributed theta networks than PFC-CC tDCS, perhaps, by targeting both anterior and posterior brain regions (see Fig. 1D). We conducted a data-driven analysis to test the hypothesis that WM improvement was associated with changes in theta networks across anterior and posterior topographies. To do this, we capitalized on the high trial count and analyzed fluctuations in WM and theta network enhancement (mean 2–5.9 Hz) over the course of the experimental session. A trial-by-trial quantification of mean changes was performed by sliding windows of 100 trials in steps of one trial across the experimental session, averaged across participants (Tort et al., 2009). After PFC-PPC tDCS, trial-by-trial fluctuations in DI WM accuracy were significantly correlated with trial-by-trial fluctuations in DI theta network synchrony across an anterior-posterior topography that aligned with the stimulated PFC-PPC network (mean $\rho = 0.368$, $p = 0.013$; Fig. 4A). After PFC-CC tDCS, significantly correlated changes in theta network synchrony were distributed more widely over the stimulated bilateral PFC *and* the right posterior topography (mean $\rho = 0.422$, $p = 0.004$; Fig. 4B). These results indicate that theta network enhancement across anterior and posterior topographies tracked tDCS-linked improvements in WM accuracy regardless of cathode placement.

3.2. Reaction time

3.2.1. Education level predicts RT improvement—

As in the analysis of WM accuracy, we first evaluated changes in RT without considering individual differences. DI RT scores were subjected to a repeated measures ANOVA compared to zero including the within-subjects factors of montage (PFC-PPC, PFC-CC), set size (1, 3), and quartile (Q1–4). No main effects or interactions reached significance ($p > 0.46$; Fig. 5A). Note that although

there was no significant effect of set size on changes in RT, analysis of the raw data again confirmed that the set size manipulation was effective across tDCS conditions, including sham (paired *t*-test $p < 0.001$; Fig. S1B).

After incorporating individual difference covariates (education, age, MOCA, Digit Span, OSpan, CORSI), a main effect of tDCS montage emerged, pointing to a general benefit of PFC-PPC tDCS on RT ($F_{1, 462} = 14.39$, $p < 0.001$, $\eta^2_p = 0.03$). There was a significant contribution of education ($F_{1, 462} = 11.81$, $p < 0.001$, $\eta^2_p = 0.03$), again demonstrating that *individuals with more education showed greater RT improvement* after tDCS (Fig. 5B). In addition, there was a significant negative association with MOCA score ($F_{1, 462} = 18.10$, $p = < 0.001$, $\eta^2_p = 0.04$) and a MOCA × montage interaction ($F_{1, 462} = 8.02$, $p = 0.005$, $\eta^2_p = 0.02$), demonstrating that PFC-CC tDCS benefitted participants with higher MOCA scores (Fig. 5C, left). Last, an age × montage interaction ($F_{1, 462} = 12.79$, $p < 0.001$, $\eta^2_p = 0.03$) demonstrated that younger OA participants responded faster after PFC-PPC tDCS whereas older participants responded faster after PPC-CC tDCS (Fig. 5C, right). No other effects reached significance ($p > 0.11$).

3.2.2. Theta-gamma PAC tracks RT improvement in OA independent of education—

Having demonstrated inter-individual differences in tDCS-linked RT improvement, we again sought underlying neural correlates. Unlike the WM accuracy results, neither of the correlations between DI RT and DI theta network synchrony scores was significant ($p > 0.08$). However, both cluster-corrected correlations between DI RT and DI PAC scores were significant (PFC-PPC mean $\rho = 0.377$, $p = 0.04$; PFC-CC mean $\rho = 0.383$, $p = 0.034$; Fig. 6). The behavioral benefits were characterized by increased PAC between phase at the PFC anodal site in the theta range (PFC-PPC: 4.9–10.0 Hz; PFC-CC: 2–3.4 Hz) and broadband gamma activity near cathodal sites. With both montages, the topographical distribution of significant effects reflected the direction of tDCS current flow. There were no significant correlations with ERSPs ($p > 0.1$).

As in the analysis of WM accuracy (see Section 3.1.2), post hoc multiple regression analyses examined whether changes in theta-gamma PAC and RT were moderated by an individual's education level. Here, however, the interaction was not significant for either montage ($p > 0.62$). Collectively, these results indicate that tDCS sped up RT by strengthening theta-gamma PAC in the direction of current flow in OA independent of education level.

3.2.3. RT and theta-gamma PAC changes predict WM changes in OA independent of education—

Last, we investigated whether improved RT contributed to improved WM. This prospect was supported by a significant negative correlation between WM and RT improvements, collapsed across montages ($\rho = -0.51$, $p = 0.004$). However, dissociable education effects between the theta network signature of WM improvement (see Section 3.1.2) and theta-gamma PAC signature of RT improvement (see Section 3.2.2) suggested that RT improvement may contribute to WM improvement independent of education. We conducted a multiple regression analysis to test the hypothesis that WM improvement was associated with changes in RT and theta-gamma PAC and, if so, whether the effect was independent of theta network enhancement in OA with more education. The PFC-PPC tDCS model revealed significant interactions of both DI RT × DI theta-gamma

PAC ($t = -2.55$, $p = 0.023$, $b = -19.27$, 95% CI = [−140.92, 44.79]; Fig. 7A) and education × DI theta network synchrony ($t = 3.89$, $p = 0.002$, $b = 1.40$, 95% CI = [−0.86, 7.64]). No other interactions reached significance ($p > 0.13$), suggesting that these interactions were independent. The equivalent PFC-CC tDCS model, including the subthreshold network signature of improvements in WM accuracy, revealed a significant DI RT × DI theta-gamma PAC interaction ($t = 2.18$, $p = 0.047$, $b = 39.61$, 95% CI = [−47.73, 250.70]; Fig. 7B). No other interactions reached significance ($p > 0.19$). With both tDCS montages, RT improvement and enhanced theta-gamma PAC predicted WM improvement in OA, and the effect was independent of education.

To recapitulate, results show that tDCS improved WM by 1) strengthening theta networks, particularly in OA with more education; *and* 2) speeding RT and enhancing theta-gamma PAC, independent of education. Education, changes in RT, and changes in theta network synchrony and theta-gamma PAC together explained 68–70% of inter-individual variability in tDCS-linked improvement in WM accuracy.

4. Discussion

The rapidly growing population of OA provides incentive to establish safe, effective, affordable ways to maintain WM in aging (Scott et al., 2021). Noninvasive neurostimulation approaches offer themselves as intervention but fall short in delivering reliable behavioral benefits across participants (Berryhill and Martin, 2018). We investigated two impediments blocking widespread implementation: poor ability to predict who will respond to tDCS and poor understanding of the neural mechanisms by which tDCS improves WM. To the first point, when considering multiple individual factors (education, WM span, etc.), education emerged as a reliable and readily available demographic factor predicting tDCS efficacy. This finding extends our earlier work (Berryhill and Jones, 2012) by showing that an OA's education level predicts tDCS efficacy regardless of the specific montage. Considering the broader literature, not only are highly educated OA more resilient than less educated OA to age-related declines in brain health and cognition (Chan et al., 2021), but they are also more receptive to intervention by means of one-dose tDCS.

To the second point, individual WM improvements were associated with two distinct electrophysiological signatures implicating inter-regional interactions across spatial and temporal scales. A broad enhancement of theta networks tracked improvements in behavioral accuracy after PFC-PPC tDCS, particularly in OA with more education. Further data-driven analyses revealed that accuracy dynamics reflected an anterior-posterior network distribution regardless of cathode placement, consistent with the involvement of frontoparietal theta networks in WM (de Vries et al., 2020; Helfrich and Knight, 2016; Johnson et al., 2017, 2019; Mamashli et al., 2021; Parto Dezfouli et al., 2021). Our findings underscore the importance of theta network synchrony to WM performance (Alekseichuk et al., 2017; Reinhart et al., 2017a) and replicate observations that it can be enhanced with noninvasive neurostimulation (Jones et al., 2017; Reinhart and Nguyen, 2019). Because the effect was robust with PFC-PPC tDCS but not PFC-CC tDCS, it is likely that near-exclusive use of montages targeting PFC are suboptimal for WM. Rather, interventions seeking to improve WM in OA should target both anterior and posterior brain regions for maximal

benefits across the population. In OA, this approach preferentially targets posterior brain regions showing less activity with age (Davis et al., 2008).

In contrast, specific enhancements of theta-gamma PAC reflecting PFC-PPC and PFC-CC tDCS current flow tracked individual improvements in RT. This finding extends observations that PAC can be enhanced with noninvasive neurostimulation (Alekseichuk et al., 2016; Jones et al., 2020a,b; Reinhart and Nguyen, 2019). Post hoc analyses revealed that, unlike the relationship between WM accuracy and theta networks, relationships between RT and theta-gamma PAC were independent of education. Indeed, changes in RT and theta-gamma PAC together explained inter-individual variability in WM improvement independent of education, suggesting an alternate route by which tDCS could benefit OA with less education. Taken together, our findings illuminate anterior-posterior theta networks and theta-gamma PAC and as distinct but complementary signatures of WM enhancement in OA.

4.1. Why do the ‘rich get richer’?

We replicated the finding that an OA’s education level predicts tDCS efficacy (e.g., Berryhill and Jones, 2012), but failed to replicate observations that standardized measures of WM span would reliably predict tDCS efficacy (Arciniega et al., 2018). Even in this well-educated sample, the rich (highly educated) got richer (more WM improvement). Years of education is an easy measure to collect as it requires no testing. Ascertaining *why* education predicts tDCS efficacy, however, is more challenging. We can only speculate that the underlying reason is multifactorial. Education is linked to varied protective factors, and/or a lifetime of practice flexibly engaging brain networks. Indeed, high education is associated with lifelong success, reflects socioeconomic status, and is considered a proxy measure of brain and cognitive reserves with cognitive ability persisting longer in the presence of pathological change in more educated individuals (Stern et al., 2019). Indeed, OA with more education are more resilient than those with less education to age-related declines in brain health, as indexed by functional brain networks (Chan et al., 2021). Based on our theta network findings, we propose a link between an individual’s brain health and tDCS efficacy which is predicted by education level. Supporting this proposal, baseline resting-state functional connectivity has been shown to predict tDCS effects in young adults (Cerreta et al., 2020). Future research may tease apart what aspects of education, and potentially other factors of cognitive reserve, contribute to tDCS responsivity in OA.

Although the education effect demonstrates that the rich are likely to get richer, that is not the only explanation of tDCS-linked WM improvement we observed. This is important because a benefit of tDCS is its low risk and cost (Berryhill, 2017; Berryhill and Martin, 2018), which makes it feasible for widespread implementation across rich *and* less rich OA. Models of individual predictors and electrophysiological signatures of WM enhancement revealed that tDCS could also improve WM by speeding RT and enhancing theta-gamma PAC. The interaction was significant in models of both PFC-PPC and PFC-CC tDCS effects, and it was independent of education. These results suggest a circuitous path by which tDCS could improve WM in OA without robust effects on theta networks and regardless of education level. Future research in larger samples that include less educated OA will

need to examine the full factorial effects by which tDCS can tap into theta network and/or theta-gamma PAC mechanisms to improve WM in subgroups of OA.

4.2. Limitations

These data mark a major step forward in understanding how tDCS affects behavior. However, although we provide important insight based on individual behavioral and EEG data, our results cannot speak to the genetic, cellular, or molecular mechanisms contributing to tDCS effects (Polanía et al., 2018). Indeed, we previously observed non-linear patterns of tDCS-linked WM improvements in OA as a function of genetic polymorphism (Stephens et al., 2017), substantiating the role of individual factors which extend beyond the scope of the present study. Another limitation is the underrepresentation of less educated OA (< 12 years of school), skewing the distribution of our sample to miss factors which might predict tDCS efficacy in OA without a high school degree. Future testing of larger, more representative samples is needed. Finally, given the observed importance of theta activity to WM, transcranial alternating current stimulation presents an alternative neuromodulatory approach that directly targets oscillations, but only when tailored per individual OA (Reinhart and Nguyen, 2019; Zanto et al., 2021). This is an especially important point in studies targeting OA as neural oscillations exhibit marked variability in aging (Prichep et al., 2006). The high safety and low technical hurdles associated with tDCS make it especially attractive for translational ease and scalability, without the need to tailor stimulation parameters.

4.3. Conclusion

We report that one session of tDCS improves WM in OA by tapping into two distinct but complementary mechanisms of task performance, anterior-posterior theta network synchrony and theta-gamma PAC. Thus, in heathy OA at risk of cognitive decline, a benefit of tDCS to WM may be in strengthening functional brain networks that naturally weaken during aging (Courtney and Hinault, 2021). Our findings inform models of the electrophysiological basis of WM in aging and serve to identify target mechanisms for interventions involving tDCS. In OA with high education, one session of tDCS targeting anterior and posterior regions may be sufficient to enhance WM by strengthening theta networks. In a partially overlapping sample with or without high education, one session of tDCS may still enhance WM by speeding RT and strengthening theta-gamma PAC. In other OA, multi-session tDCS may be needed (Berryhill, 2017; Berryhill and Martin, 2018; Jones et al., 2015b). Our data extend a growing literature reporting that one neuro-modulation protocol does not fit all participants, and set the stage for applied research in more vulnerable populations (e.g., mild cognitive impairment, Alzheimer's disease, neuropsychiatric disorders), in whom a better understanding of how to rescue WM is needed (Ciullo et al., 2020; Serrano et al., 2020).

Supplementary Material

Refer to Web version on PubMed Central for supplementary material.

Acknowledgements

We thank Dr. Candance Peacock for assistance. This material is based on work supported in part by several funding sources including NSF OIA 1632849 (MEB), NSF OIA 1632738 (MEB), NINDS R00 NS115918 (ELJ), and DSPAN NINDS F99/K00 NS113419 (HA). EEG facilities are supported by the National Institutes of Health (NIGMS COBRE P20 GM103650). Funding sources had no role in the study design; collection, analysis and interpretation of data; writing of the report; or decision to submit the article for publication.

Data and code availability

De-identified data and custom-built MATLAB codes are available at https://osf.io/k3xce.

References

Alekseichuk I, Pabel SC, Antal A, Paulus W, 2017. Intrahemispheric theta rhythm desynchronization impairs working memory. Restor. Neurol. Neurosci 35, 147–158. [PubMed: 28059806]

Alekseichuk I, Turi Z, Amador de Lara G, Antal A, Paulus W, 2016. Spatial Working Memory in Humans Depends on Theta and High Gamma Synchronization in the Prefrontal Cortex. Curr. Biol 26, 1513–1521. [PubMed: 27238283]

Arciniega H, Gozenman F, Jones KT, Stephens JA, Berryhill ME, 2018. Frontoparietal tDCS Benefits Visual Working Memory in Older Adults With Low Working Memory Capacity. Front Aging Neurosci. 10, 57. [PubMed: 29593522]

Arciniega H, Kilgore-Gomez A, Harris A, Peterson DJ, McBride J, Fox E, Berryhill ME, 2019. Visual working memory deficits in undergraduates with a history of mild traumatic brain injury. Attention. Perception Psychophys 81, 2597–2603.

Arciniega H, Kilgore-Gomez A, McNerney WM, Lane S, Berryhill ME, 2020. Loss of consciousness, but not etiology, predicts better working memory performance years after concussion. J. Clin. Transl. Res.

Arciniega H, Shires J, Furlong S, Kilgore-Gomez A, Cerreta A, Murray NG, Berryhill ME, 2021. Impaired visual working memory and reduced connectivity in undergraduates with a history of mild traumatic brain injury. Sci. Rep 11, 2789. [PubMed: 33531546]

Battiston F, Amico E, Barrat A, Bianconi G, Ferraz de Arruda G, Franceschiello B, Iacopini I, Kéfi S, Latora V, Moreno Y, Murray MM, Peixoto TP, Vaccarino F, Petri G, 2021. The physics of higher-order interactions in complex systems. Nat. Phys 17, 1093–1098.

Berryhill ME, 2017. Longitudinal tDCS: consistency across Working Memory Training Studies. AIMS Neurosci. 4, 71–86.

Berryhill ME, Jones KT, 2012. tDCS selectively improves working memory in older adults with more education. Neurosci. Lett 521, 148–151. [PubMed: 22684095]

Berryhill ME, Martin D, 2018. Cognitive Effects of Transcranial Direct Current Stimulation in Healthy and Clinical Populations: an Overview. J. ECT 34, e25–e35. [PubMed: 30095685]

Berryhill ME, Wencil EB, Branch Coslett H, Olson IR, 2010. A selective working memory impairment after transcranial direct current stimulation to the right parietal lobe. Neurosci. Lett 479, 312–316. [PubMed: 20570713]

Brainard DH, 1997. The psychophysics toolbox. Spat. Vis 10, 433–436. [PubMed: 9176952]

Brooks SJ, Mackenzie-Phelan R, Tully J, Schioth HB, 2020. Review of the Neural Processes of Working Memory Training: controlling the Impulse to Throw the Baby Out With the Bathwater. Front. Psychiatry 11, 512761. [PubMed: 33132926]

Buckner RL, 2004. Memory and executive function in aging and AD: multiple factors that cause decline and reserve factors that compensate. Neuron 44, 195–208. [PubMed: 15450170]

Cabeza R, 2001. Cognitive neuroscience of aging: contributions of functional neuroimaging. Scand. J. Psychol 42, 277–286. [PubMed: 11501741]

Cerreta AGB, Mruczek REB, Berryhill ME, 2020. Predicting Working Memory Training Benefits From Transcranial Direct Current Stimulation Using Resting-State fMRI. Front. Psychol 11, 570030. [PubMed: 33154728]

Chan MY, Han L, Carreno CA, Zhang Z, Rodriguez RM, LaRose M, Hassenstab J, Wig GS, 2021. Long-term prognosis and educational determinants of brain network decline in older adult individuals. Nature Aging 1, 1053–1067.

Ciullo V, Spalletta G, Caltagirone C, Banaj N, Vecchio D, Piras F, Piras F, 2020. Transcranial Direct Current Stimulation and Cognition in Neuropsychiatric Disorders: systematic Review of the Evidence and Future Directions. Neuroscientist, 1073858420936167.

Cohen MX, 2015. Comparison of different spatial transformations applied to EEG data: a case study of error processing. Int. J. Psychophysiol 97, 245–257. [PubMed: 25455427]

Courtney SM, Hinault T, 2021. When the time is right: temporal dynamics of brain activity in healthy aging and dementia. Prog. Neurobiol 203, 102076. [PubMed: 34015374]

Davis SW, Dennis NA, Daselaar SM, Fleck MS, Cabeza R, 2008. Que PASA? The posterior-anterior shift in aging. Cereb. Cortex 18, 1201–1209. [PubMed: 17925295]

de Vries IEJ, Slagter HA, Olivers CNL, 2020. Oscillatory Control over Representational States in Working Memory. Trends Cogn. Sci 24, 150–162. [PubMed: 31791896]

Filmer HL, Dux PE, Mattingley JB, 2014. Applications of transcranial direct current stimulation for understanding brain function. Trends Neurosci. 37, 742–753. [PubMed: 25189102]

Finn ES, Rosenberg MD, 2021. Beyond fingerprinting: choosing predictive connectomes over reliable connectomes. Neuroimage 239, 118254. [PubMed: 34118397]

Gan T, Nikolin S, Loo CK, Martin DM, 2019. Effects of High-Definition Transcranial Direct Current Stimulation and Theta Burst Stimulation for Modulating the Posterior Parietal Cortex. J. Int. Neuropsychol. Soc 25, 972–984. [PubMed: 31397255]

Gandiga PC, Hummel FC, Cohen LG, 2006. Transcranial DC stimulation (tDCS): a tool for double-blind sham-controlled clinical studies in brain stimulation. Clin. Neurophysiol 117, 845–850. [PubMed: 16427357]

He B, Sohrabpour A, Brown E, Liu Z, 2018. Electrophysiological Source Imaging: a Noninvasive Window to Brain Dynamics. Annu. Rev. Biomed. Eng 20, 171–196. [PubMed: 29494213]

Helfrich RF, Knight RT, 2016. Oscillatory Dynamics of Prefrontal Cognitive Control. Trends Cogn. Sci 20, 916–930. [PubMed: 27743685]

Hipp JF, Siegel M, 2013. Dissociating neuronal gamma-band activity from cranial and ocular muscle activity in EEG. Front. Hum. Neurosci 7.

Huang Y, Datta A, Bikson M, Parra LC, 2018. ROAST: an Open-Source, Fully-Automated, Realistic Volumetric-Approach-Based Simulator For TES. Conf. Proc. IEEE Eng. Med. Biol. Soc 2018, 3072–3075.

Johnson EL, Dewar CD, Solbakk AK, Endestad T, Meling TR, Knight RT, 2017. Bidirectional Frontoparietal Oscillatory Systems Support Working Memory. Curr. Biol 27, 1829–1835. [PubMed: 28602658]

Johnson EL, King-Stephens D, Weber PB, Laxer KD, Lin JJ, Knight RT, 2019. Spectral Imprints of Working Memory for Everyday Associations in the Frontoparietal Network. Front. Syst. Neurosci 12.

Jones KT, Berryhill ME, 2012. Parietal contributions to visual working memory depend on task difficulty. Front. Psychiatry 3, 81. [PubMed: 22973241]

Jones KT, Gozenman F, Berryhill ME, 2015a. The strategy and motivational influences on the beneficial effect of neurostimulation: a tDCS and fNIRS study. Neuroimage 105, 238–247. [PubMed: 25462798]

Jones KT, Johnson EL, Berryhill ME, 2020a. Frontoparietal theta-gamma interactions track working memory enhancement with training and tDCS. Neuroimage 211, 116615. [PubMed: 32044440]

Jones KT, Johnson EL, Tauxe ZS, Rojas DC, 2020b. Modulation of auditory gamma-band responses using transcranial electrical stimulation. J. Neurophysiol 123, 2504–2514. [PubMed: 32459551]

Jones KT, Peterson DJ, Blacker KJ, Berryhill ME, 2017. Frontoparietal neurostimulation modulates working memory training benefits and oscillatory synchronization. Brain Res. 1667, 28–40. [PubMed: 28502585]

Jones KT, Stephens JA, Alam M, Bikson M, Berryhill ME, 2015b. Longitudinal neurostimulation in older adults improves working memory. PLoS One 10, e0121904. [PubMed: 25849358]

Kim K, Sherwood MS, McIntire LK, McKinley RA, Ranganath C, 2021. Transcranial Direct Current Stimulation Modulates Connectivity of Left Dorsolateral Prefrontal Cortex with Distributed Cortical Networks. J. Cogn. Neurosci 33, 1381–1395. [PubMed: 34496406]

Krakauer JW, Ghazanfar AA, Gomez-Marin A, MacIver MA, Poeppel D, 2017. Neuroscience Needs Behavior: correcting a Reductionist Bias. Neuron 93, 480–490. [PubMed: 28182904]

Lachaux JP, Rodriguez E, Martinerie J, Varela FJ, 1999. Measuring phase synchrony in brain signals. Hum. Brain Mapp 8, 194–208. [PubMed: 10619414]

Lai M, Demuru M, Hillebrand A, Fraschini M, 2018. A comparison between scalp- and source-reconstructed EEG networks. Sci. Rep 8, 1–8. [PubMed: 29311619]

Luft CDB, Zioga I, Bhattacharya J, 2018. Anodal transcranial direct current stimulation (tDCS) boosts dominant brain oscillations. Brain Stimul. 11, 660–662. [PubMed: 29525236]

Mamashli F, Khan S, Hämäläinen M, Jas M, Raij T, Stufflebeam SM, Nummenmaa A, Ahveninen J, 2021. Synchronization patterns reveal neuronal coding of working memory content. Cell Rep. 36, 109566. [PubMed: 34433024]

Maris E, Oostenveld R, 2007. Nonparametric statistical testing of EEG- and MEG-data. J. Neurosci. Methods 164, 177–190. [PubMed: 17517438]

Martin A, Meinzer M, Lindenberg R, Sieg MM, Nachtigall L, Floel A, 2017. Effects of Transcranial Direct Current Stimulation on Neural Network Structure in Young and Older Adults. J. Cogn. Neurosci 1–12.

Medina J, Cason S, 2017. No evidential value in samples of transcranial direct current stimulation (tDCS) studies of cognition and working memory in healthy populations. Cortex 94, 131–141. [PubMed: 28759803]

Mezger E, Rauchmann BS, Brunoni AR, Bulubas L, Thielscher A, Werle J, Mortazavi M, Karali T, Stöcklein S, Ertl-Wagner B, Goerigk S, Padberg F, Keeser D, 2019. Effects of prefrontal cathodal tDCS on brain glutamate levels and resting state connectivity: a randomized, sham-controlled, cross-over trial in healthy volunteers. Clin. Neurophysiol 131, e127.

Nilsson J, Lebedev AV, Lovden M, 2015. No Significant Effect of Prefrontal tDCS on Working Memory Performance in Older Adults. Front. Aging Neurosci 7, 230. [PubMed: 26696882]

Nissim NR, Moberg PJ, Hamilton RH, 2020. Efficacy of Noninvasive Brain Stimulation (tDCS or TMS) Paired with Language Therapy in the Treatment of Primary Progressive Aphasia: an Exploratory Meta-Analysis. Brain Sci. 10.

Nissim NR, O'Shea A, Indahlastari A, Telles R, Richards L, Porges E, Cohen R, Woods AJ, 2019. Effects of in-Scanner Bilateral Frontal tDCS on Functional Connectivity of the Working Memory Network in Older Adults. Front. Aging Neurosci 11, 51. [PubMed: 30930766]

Nitsche MA, Paulus W, 2001. Sustained excitability elevations induced by transcranial DC motor cortex stimulation in humans. Neurology 57, 1899–1901. [PubMed: 11723286]

Nuechterlein KH, Green MF, Kern RS, Baade LE, Barch DM, Cohen JD, Essock S, Fenton WS, Frese III FJ, Gold JM, Goldberg T, Heaton RK, Keefe RSE, Kraemer H, Mesholam-Gately R, Seidman LJ, Stover E, Weinberger DR, Young AS, Zalcman SR, Marder SR, 2008. The MATRICS consensus cognitive battery, part 1: test selection, reliability, and validity. Am. J. Psychiatry 165, 203–213. [PubMed: 18172019]

Oostenveld R, Fries P, Maris E, Schoffelen J-M, 2011. FieldTrip: open source software for advanced analysis of MEG, EEG, and invasive electrophysiological data. Comput. Intell. Neurosci 2011.

Park DC, Lautenschlager G, Hedden T, Davidson NS, Smith AD, Smith PK, 2002. Models of visuospatial and verbal memory across the adult life span. Psychol. Aging 17, 299–320. [PubMed: 12061414]

Parto Dezfouli M, Davoudi S, Knight RT, Daliri MR, Johnson EL, 2021. Prefrontal lesions disrupt oscillatory signatures of spatiotemporal integration in working memory. Cortex 138, 113–126. [PubMed: 33684625]

Penny WD, Duzel E, Miller KJ, Ojemann JG, 2008. Testing for nested oscillation. J. Neurosci. Methods 174, 50–61. [PubMed: 18674562]

Polanía R, Nitsche MA, Ruff CC, 2018. Studying and modifying brain function with non-invasive brain stimulation. Nat. Neurosci 21, 174–187. [PubMed: 29311747]

Prichep LS, John ER, Ferris SH, Rausch L, Fang Z, Cancro R, Torossian C, Reisberg B, 2006. Prediction of longitudinal cognitive decline in normal elderly with subjective complaints using electrophysiological imaging. Neurobiol. Aging 27, 471–481. [PubMed: 16213630]

Reinhart RM, Cosman JD, Fukuda K, Woodman GF, 2017a. Using transcranial direct-current stimulation (tDCS) to understand cognitive processing. Atten. Percept. Psychophys 79, 3–23. [PubMed: 27804033]

Reinhart RM, Zhu J, Park S, Woodman GF, 2015. Synchronizing theta oscillations with direct-current stimulation strengthens adaptive control in the human brain. Proc. Natl. Acad. Sci. U. S. A 112, 9448–9453. [PubMed: 26124116]

Reinhart RMG, Cosman JD, Fukuda K, Woodman GF, 2017b. Using transcranial direct-current stimulation (tDCS) to understand cognitive processing. Attention. Perception Psychophys 79, 3–23.

Reinhart RMG, Nguyen JA, 2019. Working memory revived in older adults by synchronizing rhythmic brain circuits. Nat. Neurosci 22, 820–827. [PubMed: 30962628]

Reuter-Lorenz PA, Sylvester C-YC, 2005. The Cognitive Neuroscience of Working Memory and Aging. Cognitive neuroscience of aging: Linking cognitive and Cerebral Aging. Oxford University Press, New York, NY, US, pp. 186–217.

Salat DH, Buckner RL, Snyder AZ, Greve DN, Desikan RS, Busa E, Morris JC, Dale AM, Fischl B, 2004. Thinning of the cerebral cortex in aging. Cereb. Cortex 14, 721–730. [PubMed: 15054051]

Scott AJ, Ellison M, Sinclair DA, 2021. The economic value of targeting aging. Nature Aging 1, 616–623.

Serrano N, Lopez-Sanz D, Bruna R, Garces P, Rodriguez-Rojo IC, Marcos A, Crespo DP, Maestu F, 2020. Spatiotemporal Oscillatory Patterns During Working Memory Maintenance in Mild Cognitive Impairment and Subjective Cognitive Decline. Int. J. Neural Syst 30, 1950019. [PubMed: 31522594]

Sporns O, 2018. Graph theory methods: applications in brain networks. Dialogues Clin. Neurosci 20, 111–121. [PubMed: 30250388]

Stephens JA, Jones KT, Berryhill ME, 2017. Task demands, tDCS intensity, and the COMT val(158)met polymorphism impact tDCS-linked working memory training gains. Sci. Rep 7, 13463. [PubMed: 29044248]

Stern Y, Barnes CA, Grady C, Jones RN, Raz N, 2019. Brain reserve, cognitive reserve, compensation, and maintenance: operationalization, validity, and mechanisms of cognitive resilience. Neurobiol. Aging 83, 124–129. [PubMed: 31732015]

Tort ABL, Komorowski RW, Manns JR, Kopell NJ, Eichenbaum H, 2009. Theta–gamma coupling increases during the learning of item–context associations. Proc. Natl. Acad. Sci 106, 20942. [PubMed: 19934062]

Tseng P, Hsu TY, Chang CF, Tzeng OJ, Hung DL, Muggleton NG, Walsh V, Liang WK, Cheng SK, Juan CH, 2012. Unleashing Potential: transcranial Direct Current Stimulation over the Right Posterior Parietal Cortex Improves Change Detection in Low-Performing Individuals. J. Neurosci 32, 10554–10561. [PubMed: 22855805]

Unsworth N, Heitz RP, Schrock JC, Engle RW, 2005. An automated version of the operation span task. Behav. Res. Methods 37, 498–505. [PubMed: 16405146]

Vogel EK, Machlzawa MG, 2004. Neural activity predicts individual differences in visual working memory capacity. Nature 428, 748–751. [PubMed: 15085132]

Wechsler D, 2009. Wechsler Memory Scale-Fourth edition: Administration and Scoring Manual. Psychological Corporation, San Antonio, TX.

Zaehle T, Sandmann P, Thorne JD, Jancke L, Herrmann CS, 2011. Transcranial direct current stimulation of the prefrontal cortex modulates working memory performance: combined behavioural and electrophysiological evidence. BMC Neurosci. 12, 2. [PubMed: 21211016]

Zanto TP, Jones KT, Ostrand AE, Hsu W−Y, Campusano R, Gazzaley A, 2021. Individual differences in neuroanatomy and neurophysiology predict effects of transcranial alternating current stimulation. Brain Stimul. 14, 1317–1329. [PubMed: 34481095]

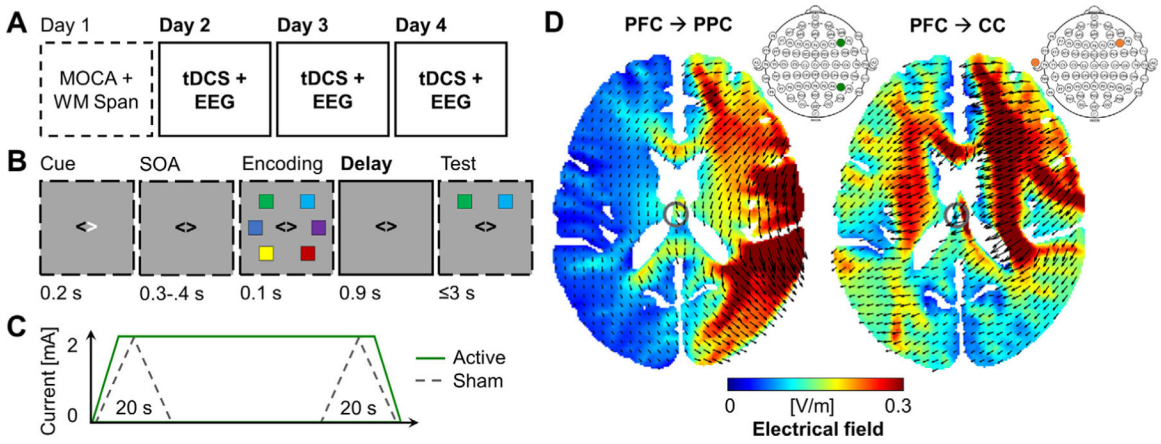

Fig. 1.

Study design. A) Study events per day of testing. Participants completed baseline testing (MOCA, Digit Span, OSpan, CORSI) and 3 tDCS sessions (PFC-PPC, PFC–CC, sham). During tDCS sessions, participants performed practice trials during stimulation, electrodes were removed, and EEG was recorded during experimental trials. Boldface identifies data analyzed. B) WM task. The change detection task trials began with fixation, followed by a cue indicating the hemifield to covertly attend. WM arrays included 1 or 3 stimuli per hemifield. After a delay, a probe appeared, and participants judged whether the color matched the color shown during encoding (match trial shown). Stimuli are not to scale. Boldface identifies data analyzed. C) TDCS protocol. During each active tDCS session, 20 min of 2 mA stimulation was applied. During sham, stimulation was applied for 20 s at the beginning and end of 20 min. Green, active; gray, sham. D) TDCS current models. TDCS was applied with the anode positioned over right PFC (F6) and the cathode over right PPC (P6; left) or contralateral cheek (CC; right). Cathode placement was counterbalanced during sham sessions. Arrows indicate current flow in the anode-to-cathode direction. Insets: anode and cathode positions on the 10–20 system.

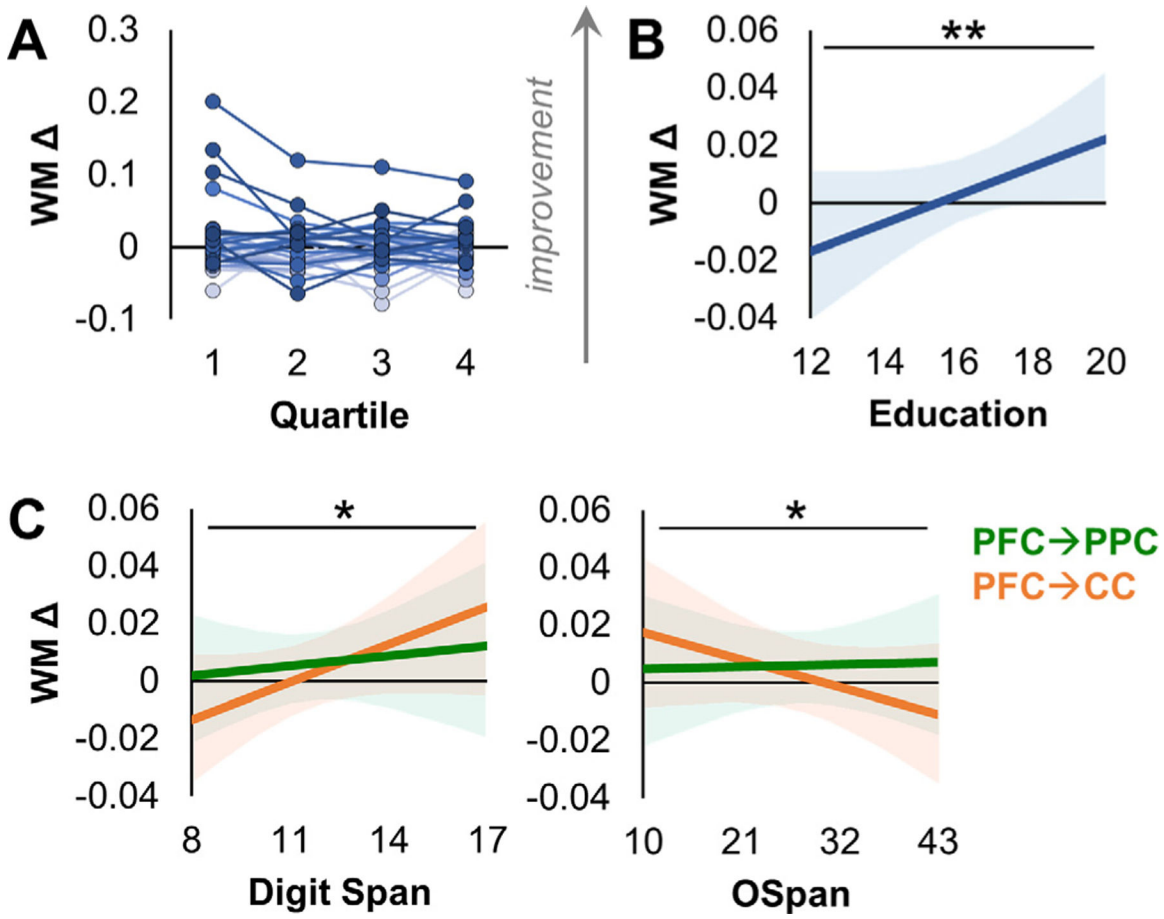

Fig. 2.

Individual differences in WM improvement. **A**) No significant tDCS effects without considering individual differences. Data are collapsed across tDCS montages and set sizes. Individual data are ordered by increasing education level on a scale from light to dark. **B**) Individual differences × education level. TDCS improved WM accuracy in individuals with higher education. Data are collapsed across set sizes and quartiles and shown as trendlines (linear fit) ± 95% CI to indicate the nature of each effect. *, $p < 0.05$; **, $p < 0.001$. **C**) Individual differences × tDCS montage. PFC-CC tDCS improved WM accuracy in participants with higher Digit Span scores (left) but lower OSpan scores (right), same conventions as (**B**).

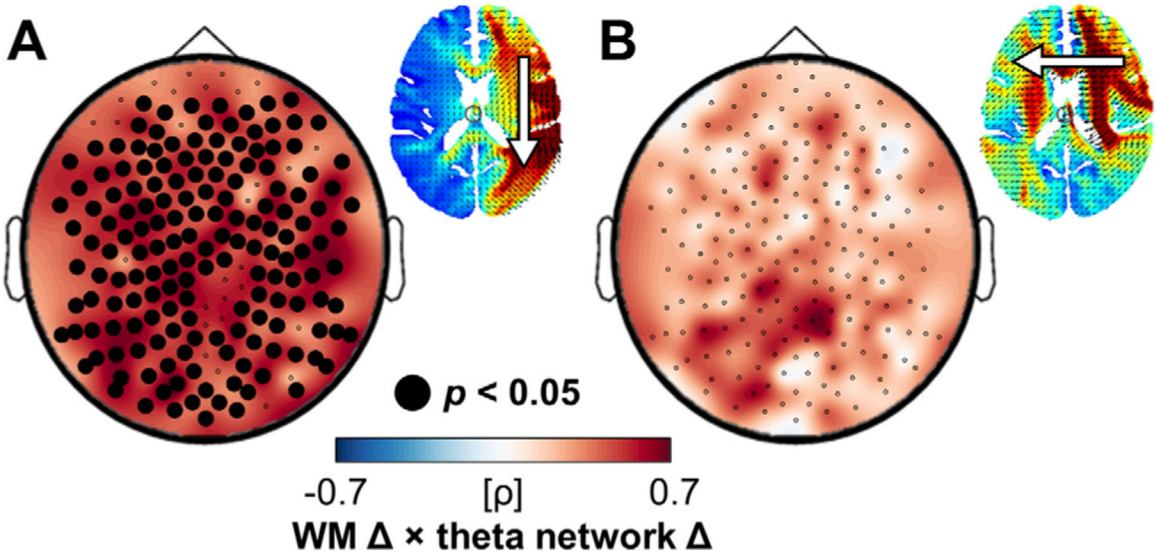

Fig. 3.

Theta network signature of individual differences in WM improvement. **A**) Participants who benefited more from PFC-PPC tDCS showed greater increases in theta network synchrony (i.e., more supra-threshold PLV connections between each channel and all other channels). Cluster-corrected correlation between changes in WM accuracy and changes in theta network synchrony relative to sham. Black circles, EEG channels that showed significant effects. Inset: tDCS current model and anode-to-cathode flow. **B**) Same as (**A**) with PFC-CC tDCS. No significant effects.

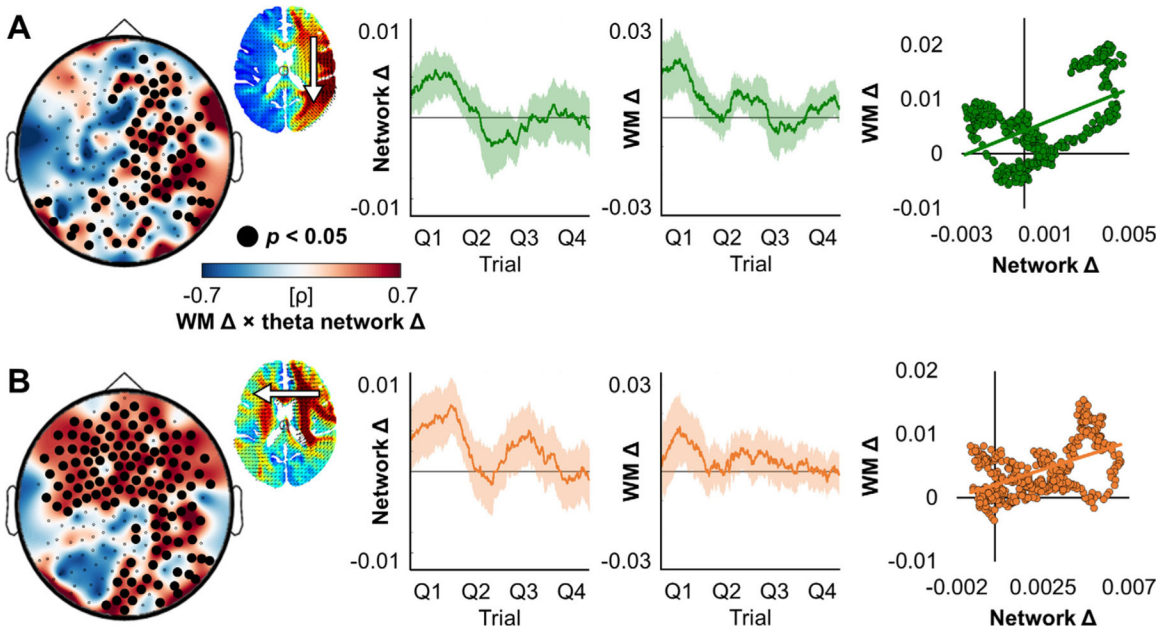

Fig. 4.

Anterior-posterior theta network signature of WM improvement. A) Changes in WM accuracy were associated with anterior and posterior theta network enhancement over the course of the experimental session. Cluster-corrected correlation between trial-by-trial DI WM accuracy and trial-by-trial DI theta network synchrony scores with PFC-PPC tDCS (left). Black circles, EEG channels that showed significant effects. Inset: tDCS current model and anode-to-cathode flow. Trial-by-trial changes in theta network synchrony and changes in WM accuracy were calculated using 100-trial sliding windows, represented as mean ± SEM relative to sham across participants (middle). The relationship is shown point by point per 100-trial window as WM changes over theta network changes (right). Data are collapsed across set sizes. B) Same as (A) with PFC-CC tDCS. With both tDCS montages, the distribution of significant effects reflects the direction of current flow (inset) and right anterior-posterior topography.

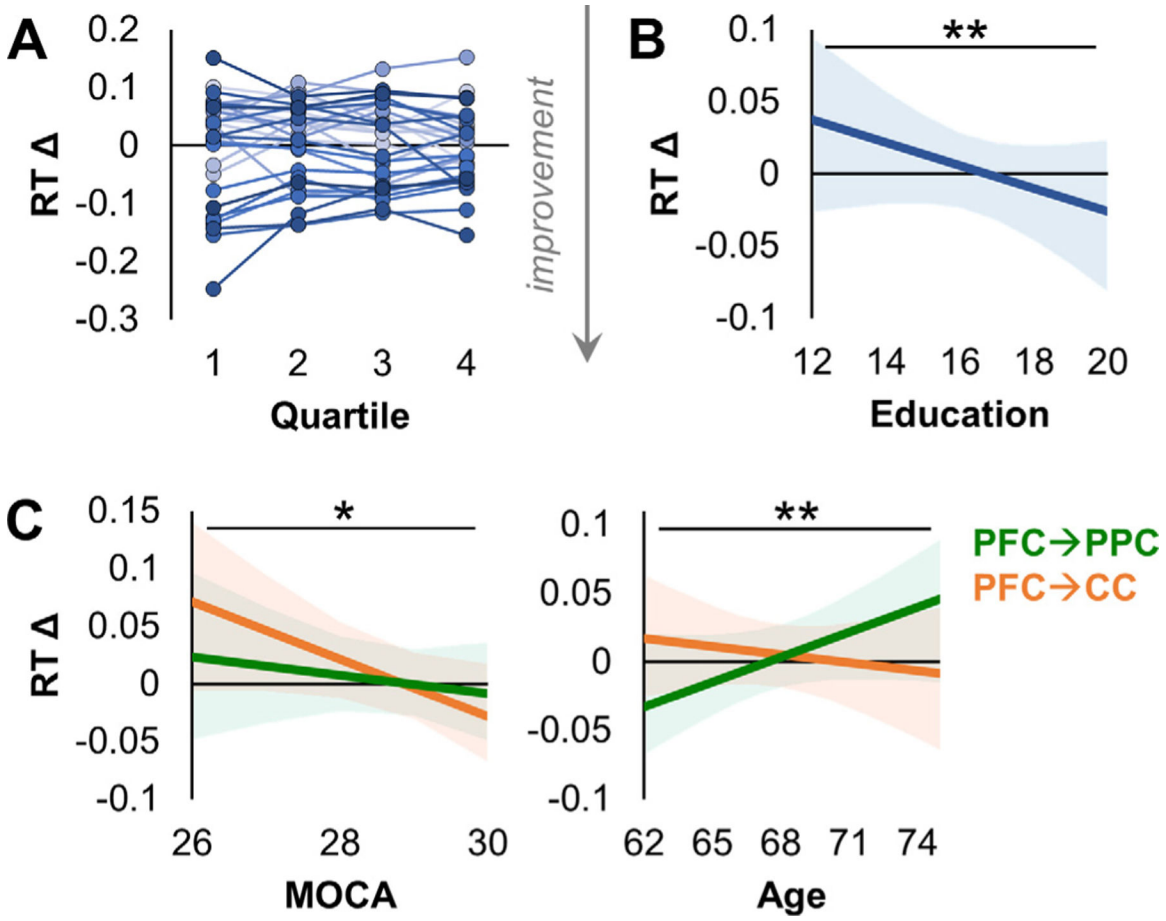

Fig. 5.

Individual differences in RT improvement. **A**) No significant tDCS effects without considering individual differences. Data are collapsed across tDCS montages and set sizes. Individual data are ordered by increasing education level on a scale from light to dark. **B**) Individual differences × education level. TDCS improved RT in individuals with higher education. Data are collapsed across set sizes and quartiles and shown as trendlines (linear fit) ± 95% CI to indicate the nature of each effect. *, $p < 0.05$; **, $p < 0.001$. **C**) Individual differences × tDCS montage. MOCA scores predicted RT improvement and the benefit was amplified with PFC-CC tDCS (left). Age predicted tDCS effects such that PFC-PPC tDCS sped up RT in individuals closer to age 60 and PFC-CC tDCS sped up RT in individuals closer to age 75 (right), same conventions as (**B**).

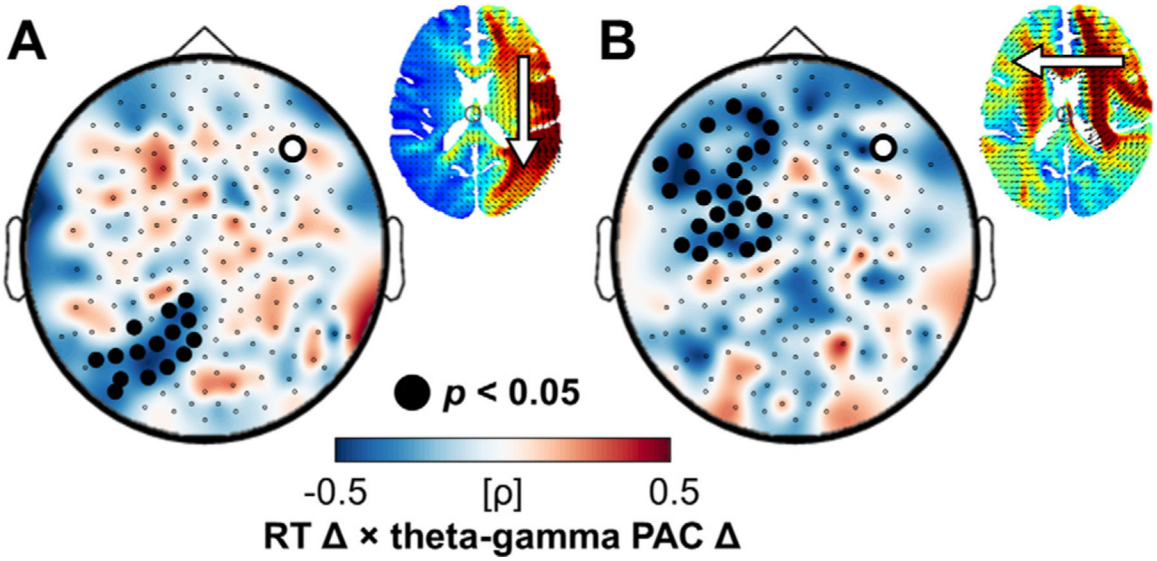

Fig. 6.

Theta-gamma PAC signature of individual differences in RT improvement. **A**) Participants who benefitted more from PFC-PPC tDCS showed greater increases in PAC between theta at the PFC anodal site (F6, marked in white) and posterior gamma. Cluster-corrected correlation between changes in RT and changes in PAC relative to sham. White circle, theta phase seed channel; black circles, gamma amplitude channels that showed significant effects. Inset: tDCS current model and anode-to-cathode flow. **B**) Same as (**A**) with PFC-CC tDCS. With both tDCS montages, the topographical distribution of significant effects reflects the direction of current flow (inset).

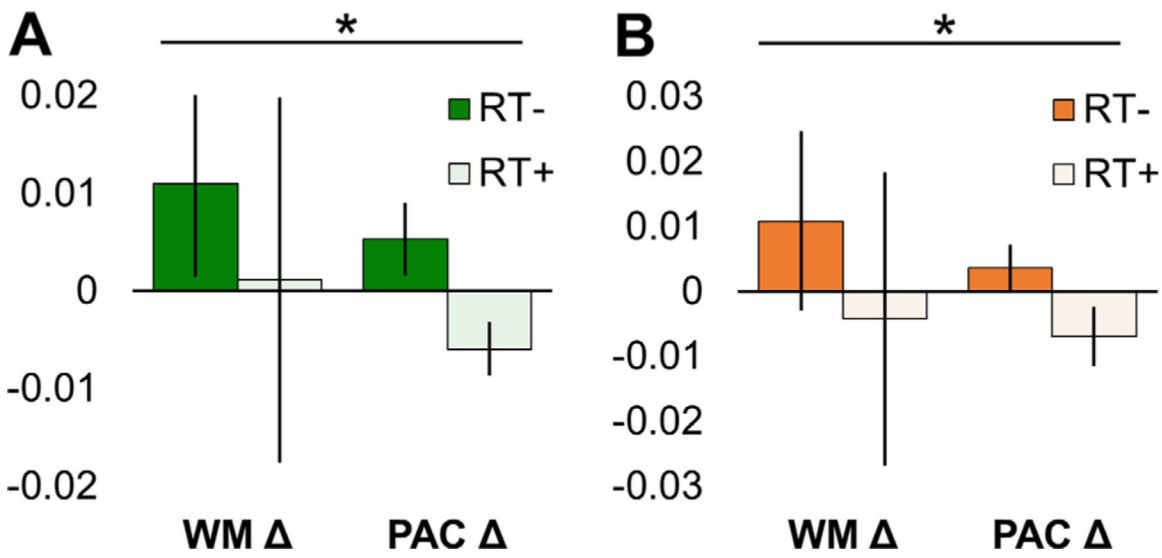

Fig. 7.

RT × theta-gamma PAC signature of WM improvement. **A**) Individual differences in WM improvement × RT and theta-gamma PAC changes. After PFC-PPC tDCS, RT improvement and enhanced theta-gamma PAC predicted WM improvement (dark green). Data are split by the direction of RT change ($n = 14$ decreased RT, i.e., improvement; $n = 16$ increased RT) and shown as means ± 95% CI to indicate the nature of the interaction. RT−, decreased RT; RT+, increased RT; *, $p < 0.05$. **B**) Same as (**A**) for PFC-CC tDCS ($n = 16$ decreased RT; $n = 14$ increased RT).